Bulk photovoltaic effect of $LiNbO_3$:Fe and its small-polaron-based microscopic interpretation

O. F. Schirmer* and M. Imlau
Universität Osnabrück, Fachbereich Physik, Osnabrück, Germany

C. Merschjann
Helmholtz-Zentrum Berlin für Materialien und Energie GmbH, Berlin, Germany

(Received 25 October 2010; revised manuscript received 5 January 2011; published 12 April 2011)

Based on recent experimental evidence on the electronic and optical properties of Fe_{Li}^{2+} and Nb_{Nb}^{4+} in $LiNbO_3$:Fe, both strongly determined by their small polaron character, a microscopic model is presented accounting for the main features of the bulk photovoltaic effect (BPVE) in this material. The relative sizes of the components of the photovoltaic tensor are explained on an atomic basis. Optical small polaron transfer from Fe_{Li}^{2+} to Nb_{Nb}^{5+} conduction band states and the subsequent coherent bandlike electron transport, terminated by the formation of Nb_{Nb}^{4+} free small polarons within about 10^{-13} s, characterize the first steps of the BPVE. These free polarons, transported by thermally activated incoherent hopping, are then trapped by deeper defects such as Nb_{Li}^{5+} and Fe_{Li}^{3+} impurities. The model allows us to explain the strong increase of the ionization probability of Fe_{Li}^{2+} and the coherent transport length with photon energy. The low mobility of the Nb_{Nb}^{4+} conduction polarons appears to be the reason for the high open-circuit photovoltaic fields attainable in $LiNbO_3$.

DOI: 10.1103/PhysRevB.83.165106 PACS number(s): 71.38.Ht, 71.38.Mx, 77.84.Ek, 78.47.jb

I. INTRODUCTION

Homogeneous illumination of the polar material $LiNbO_3$ (LN), containing Fe^{2+} defect ions on Li sites, gives rise to a steady short-circuit current.[1] Since it flows in the bulk of a uniform crystal, in the absence of spatial inhomogeneities, it is attributed to a bulk photovoltaic effect (BPVE). This is the dominating charge transport mechanism initiating the photorefractive effect in LN:Fe,[1–3] enabling a variety of optical applications, including holographic data storage,[4] phase conjugating mirrors,[5] optical filters,[6] etc. The most significant properties of LN crystals for photonic applications have been reviewed by Arizmendi.[7] Investigations into the usefulness of the photovoltaic features of ferroelectrics in general continue to be published (cf. Refs. 8–10). For an overview on bulk photovoltaic phenomena in LN and other crystals lacking a center of symmetry, see Sturman and Fridkin.[11] Various authors have discussed the physical constraints with which a BPVE must comply and proposed general phenomenological models for its formation on this basis.[1,11–16]

These studies were performed more than two decades ago. Since then, further experimental and theoretical investigations of the atomistic properties of LN have been published, which determine the optical and electronic transport features of nominally pure and impurity containing material. It was shown, for instance, that free electrons couple more strongly to the ions in $LiNbO_3$ than in any other ABO_3 compound. The related tendency of electron self-trapping is manifested by various types of free and bound small polarons. A review on this subject has been presented by Schirmer *et al.*[17] Furthermore, pump-probe absorption studies, employing ultrashort fs pulses,[18,19] have led to detailed insight into which states electrons are excited initially and by which processes they decay subsequently. The obtained increased knowledge on the relevant properties of LN allows us to approach the interpretation of the BPVE on this new basis and to address problems so far unsolved in this field. These include the following: (1) What is the microscopic reason for the strong anisotropy of the photovoltaic tensor, predicting much larger photovoltaic currents parallel to the polar *c* axis than perpendicular to it? (2) Why does the photovoltaic current rise much stronger with photon energy than the optical absorption? (3) Why are the open-circuit photovoltaic fields for $LiNbO_3$:Fe so extraordinarily high?

It is remarkable that the BPVE in LN:Fe has so far not been treated by a detailed consideration of the microscopic processes leading to its optical absorption. This approach will be the basis for our investigation, sketched by a short outline in the following. The interaction of light with Fe_{Li}^{2+} in LN is dominated by a wide and intense absorption band with an onset near 1.6 eV and a maximum near 2.6 eV. It has been attributed by Clark *et al.*[20] to Fe^{2+} substituting for Li^+ and assigned to an optical intervalence transfer transition[21] of an electron from Fe_{Li}^{2+} to neighboring Nb_{Nb}^{5+} ions. This implies that an electron, initially localized at the Fe_{Li} site by the defect potential and the surrounding self-induced lattice distortion, is excited to the final sites under Franck-Condon conditions, leading to the mentioned absorption band. As noted by Hush,[21] intervalence absorption features can also be described, in a wider context, by the small polaron formalism.[22–27] Making use of this model, we have interpreted[17] the optical absorption of Fe_{Li}^{2+} as a light-induced transition of a small polaron bound to a Fe_{Li}^{3+} defect to a neighboring Nb_{Nb}^{5+} ion. The result of this first step can also be considered as the population of excited, nonthermalized conduction band states. An electron in such states can lose its surplus energy by displacing its neighboring ions, leading to the formation of a Nb_{Nb}^{4+} free small polaron. It has a level slightly below the rigid lattice band edge. Ultrafast absorption spectroscopy has verified that the corresponding free polaron absorption band peaking near 1.0 eV forms in the time range of 10^{-13} s at room temperature.[18,19] In LN, those free polarons are stabilized by the sizable energy of 0.54 eV,[17] a value larger than in any other known ABO_3

compound. As a consequence, the transport of free conduction electrons in undoped LN, represented by such free Nb_{Nb}^{4+} free polarons, occurs by hopping between Nb_{Nb} sites, thermally activated by 0.27 eV,[17] one-half of the polaron binding energy as predicted from the theory for free small polarons.[26] Because of the high hopping activation energy in LN, the mobility μ of the conduction electrons is much less than the lower bound expected for band transport via delocalized states $\mu \geqslant 1\ \mathrm{cm}^2/\mathrm{Vs}$.[28]

The initial state of the optically excited electron is characterized, before the electron loses energy by thermalization, by the hybrid situation typical for defect states resonant with band states. On the one hand, the spatial extension of the wave amplitude of the excited electron is still determined by its localizing starting conditions, i.e., the Fe_{Li}^{3+} defect potential and the initial ligand ion displacements around the Fe_{Li}^{2+} site, which are typical for a small polaron. These excursions correspond to the formation of the Fe_{Li}^{2+} small polaron situation and are conserved approximately under Franck-Condon excitation. On the other hand, an electron in a nonrelaxed state at Nb_{Nb}^{4+}, initially created by optical excitation, will tend to tunnel to equivalent Nb_{Nb}^{5+} ions, being part of the periodic structure of the crystal. The mixture of the corresponding band states with those determined by the local potential will depend strongly on the absorbed photon energy. The probability for photoionization is expected to increase with rising energy. This relation will indeed be found to influence the dependence of the photovoltaic current on photon energy.

Taking the polaronic features as well as the structural environment in the first coordination sphere around Fe_{Li} into account, we can now understand the appearance of the photovoltaic current on an atomic basis as follows: the total optical absorption essentially results from a superposition of electron transfers from Fe_{Li}^{2+} to one of the eight surrounding nearest Nb_{Nb}^{5+} ions. Each such transfer, representing a time-dependent change of a Fe_{Li}-Nb_{Nb} dipole, can be understood as a light-induced local current. A net current with respect to a given direction, e.g., the polar c axis, will result if the related projections of all the individual dipolar currents to the eight Nb_{Nb}^{5+} neighbors do not add up to zero. As will be shown, it is an intrinsic feature of small polaron transitions that the related transfer probabilities depend strongly on the Fe_{Li}^{2+}-Nb_{Nb}^{5+} distances. For ions on Li sites, their projections on the c axis are rather unequal and therefore a sizable net current along this direction is expected. These time-dependent changes of local Fe_{Li}-Nb_{Nb} dipoles will trigger the flow of a current $\mathbf{j}$ throughout the crystal. The dependence of these changes on the directions of the exciting light electric fields relative to those of the dipoles determines the related tensorial characteristics of $\mathbf{j}$.

Following this overview, we shall first analyze these anisotropic properties of the dipole excitations. This will be the basis for the interpretation of the photovoltaic tensor, which expresses the details of the response of $\mathbf{j}$ to the light intensity I. Then, the mentioned dipole optical transfers will be viewed from a complementary approach: as transitions to the conduction band. At first, transitions to low-lying Franck-Condon excited small polaron states resonant with the conduction band will be considered. They are mainly determined by the defect potential. Subsequently, contributions arising from the admixture of band states, governed by the periodic lattice potential, will be treated. These start to dominate with rising photon energies. The resulting transport, initially coherent before being randomized by scattering, is the starting process kicking off the photovoltaic current $\mathbf{j}_{\mathrm{phv}}$. Very fast relaxation from this initial bandlike motion to the Nb_{Nb}^{4+} free polaron conduction ground states and eventually to one of the Fe_{Li} dopants, by incoherent diffusive hopping motion, will then be treated. This transport determines the photoconductivity σ_I; together with the photovoltaic current, it is responsible for the photovoltaic open circuit field $\mathbf{E}_{\mathrm{phv}}$. Its high value, up to 10^5 V/cm, will be shown to result from the low mobility of the conduction polarons.

II. THE PHOTOVOLTAIC TENSOR OF LN:Fe_{Li} AND ITS RELATION TO OPTICAL ABSORPTION

A. Properties of the photovoltaic tensor

Being a polar vector, the photovoltaic current $\mathbf{j}$ can be nonzero only in crystals lacking a center of inversion. Although $\mathbf{j}$ is strictly employed as a current density, for brevity, we shall continue to designate it as a current. Photovoltaic effects are characterized by the proportionality of the photoinduced current to the light intensity I, which is itself proportional to the squares of the incident photon electric fields $\mathbf{E} \cdot \mathbf{E}^*$. Phenomenologically, this relation can be expressed by a third-rank complex tensor β_{ikl},[29] yielding the components of the current as

$$j_i = \beta_{ikl} e_k e_l^* \cdot I, \tag{1}$$

where the components e_k, e_l^* represent unit vectors of the light electric field. We note that summation over repeated indices is implied and confine our attention here to the application of linearly polarized light. Thus, we deal with the real components of the β_{ikl} tensor only, which are symmetric in the indices k and l.[29] For LN, having the point group $3m$ below its Curie temperature (∼1400 K, depending on the Li/Nb ratio), group theory requires that there are only four independent tensor elements, which can be different from zero:[11,29,30]

$$\beta_{zzz}, \quad \beta_{zyy} = \beta_{zxx}, \tag{2}$$

$$\beta_{yyy} = -\beta_{xxy} = -\beta_{xyx} = -\beta_{yxx}, \qquad \beta_{xxz} = \beta_{xzx}^* = \beta_{yzy} = \beta_{yyz}^*. \tag{3}$$

Only the four elements in Eq. (3) can be complex by the symmetry of LN. Restricting attention to linearly polarized light, however, the possible imaginary tensor components are irrelevant. They are decisive, however, for the photorefractive hologram recording by mutually orthogonal waves.[31] For the elements in Eqs. (2) and (3), z is directed along the c axis, with y perpendicular to c (within a glide mirror plane) and x perpendicular to both in a right-handed system [see Fig. 1(a)]. The elements in Eq. (2) refer to $\mathbf{j} \parallel c$, and those in Eq. (3) to $\mathbf{j} \perp c$.

The tensorial properties of the BPVE were first verified by Fridkin and Magomadov.[32] For an Fe^{2+} concentration $c(Fe_{Li}^{2+}) = 6 \times 10^{18}\ \mathrm{cm}^{-3}$ and a photon energy of 2.48 eV

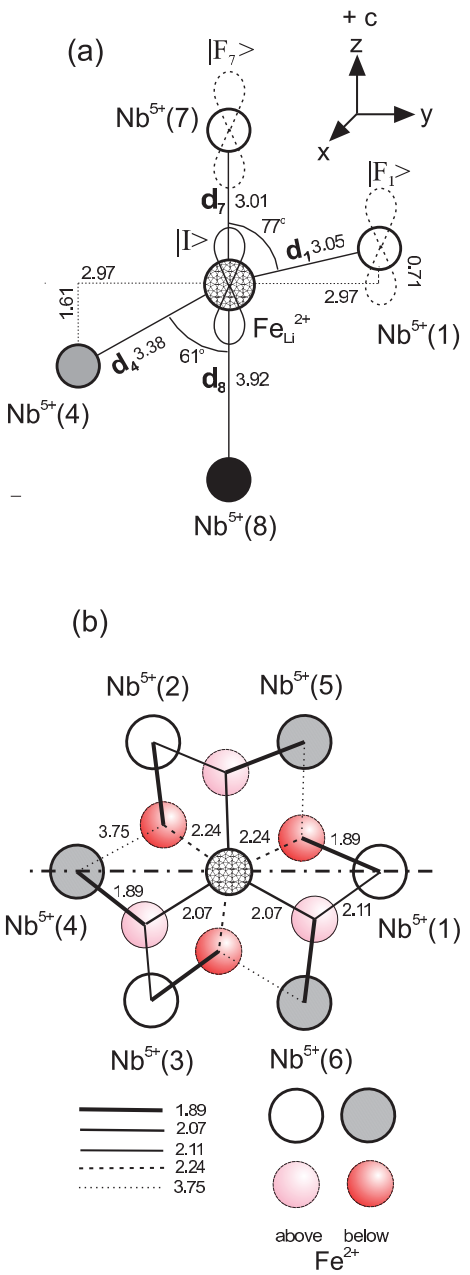

FIG. 1. (Color online) Arrangement of Fe_{Li}^{2+} and neighboring Nb_{Nb}^{5+} ions in $LiNbO_3$, assuming atomic positions unchanged with respect to the defect-free crystal. The lengths of the interionic vectors $\mathbf{d}_i$ are given in Å. (a) Cut along a yz glide mirror plane. For three sites, as examples, the axial structure (symmetry A_1 in the $3m$ group) of the involved orbitals of $(3z^2\text{-}r^2)$ type are indicated. For Fe_{Li}^{2+} $(3d^6)$, shown hatched, the orbital of the last electron is labeled $|I\rangle$. For the Nb_{Nb}^{4+} neighbors 1 and 7, they are called $|F_1\rangle$ and $|F_7\rangle$. (b) Projection on a xy plane (perpendicular to c); the trace of the glide mirror plane, along y [part (a)] is indicated by the dashed-dotted line. In this figure, the positions of the O^{2-} ions next to the shown cations and their distances to the neighboring cations are included. The thicker the connecting lines, the shorter the cation-oxygen bonds. The Fe_{Li}^{2+} ion is shown hatched. The positions of the Nb and O ions relative to the Fe_{Li}^{2+} position, i.e., above and below the xy plane, are indicated by the respective shadings (see legend).

Festl *et al.*[30] have identified $\beta_{zzz} = 40 \times 10^{-9}$ 1/V as having the same value as $\beta_{zxx} = 40 \times 10^{-9}$ 1/V at this photon energy. The values of both these elements increase linearly with energy up to 2.7 eV, above which β_{zxx} starts to dominate slightly. The value of β_{yyy} is 2×10^{-9} 1/V at 2.48 eV, rising to 6×10^{-9} 1/V at 3.0 eV. From data presented by Karabekyan,[33,34] the value of β_{xxz} can be derived to be about 0.8×10^{-9} 1/V for the Fe^{2+} concentration investigated by Festl *et al.*[30] In summary, both β_{zzz} and β_{zxx} $(=\beta_{zyy})$ [Eq. (2)], with $\mathbf{j} \parallel c$, are comparatively large and of nearly the same size, while β_{yyy} and β_{xxz} [Eq. (3)], with $\mathbf{j} \perp c$, are smaller by one to two orders of magnitude.

Karabekyan has also investigated the dependence of these four significant tensor components on photon energy.[33] An identical dispersive behavior was found; thus, all components are attributed to the same electronic transition, i.e., to the Fe-Nb intervalence transfer. The experimentally determined direction of the current flow j_z corresponds to negative charge being transported toward the $+c$ direction.[1,35]

B. Small polaron optical absorption of LN:Fe_{Li}^{2+}

Figure 1(a) indicates the relative atomic positions of Fe_{Li}^{2+} and its eight Nb_{Nb}^{5+} neighbors. We assume that Fe exactly replaces a Li site of the defect-free crystal[36] and that the structural positions of Li and Nb remain unchanged with respect to the defect-free crystal. Each of the Nb_{Nb} sites will be a possible final location of an electron transferred optically from Fe_{Li}^{2+}. A single Fe-Nb pair can thus serve as the elementary unit with which the basic facts of the absorption process can be elucidated. The orbital of the last electron in Fe_{Li}^{2+} $(3d^6)$, also having axial symmetry A_1,[37] will be symbolized by $|I\rangle$ [Fig. 1(a)]. There is a finite probability that $|I\rangle$ is leaking, via indirect coupling by O^{2-} ions [Fig. 1(b)], to each of its eight Nb_{Nb}^{5+} neighbors described by effective transfer integrals J_i (index $i = 1, \ldots, 8$). In Appendix A, it is outlined as to how the absorption $\alpha_i(\hbar\omega)$ depends on the distances d_i between Fe_{Li}^{2+} and Nb_{Nb}^{5+}, on J_i and on photon energy $\hbar\omega$:

$$\alpha_i(\hbar\omega) \sim d_i^2 J_i^2 / \omega \cdot \exp[-w(\hbar\omega - 2E_P' - E_C)^2] \qquad (4)$$

$(w^{-1} = 4E_P'\hbar\omega_0$; $\hbar\omega_0$ is the representative phonon energy; E_P' is the polaron binding energy due to lattice distortion around Fe_{Li}^{2+}; and E_C is the electronic energy shift caused by the Fe_{Li} defect potential). The observed optical absorption band of Fe_{Li}^{2+} near 2.6 eV (Fig. 2) is described by $\sum_i \alpha_i$. All $\alpha_i(\omega)$ are assumed to have identical dispersion (ω dependence) because the energy differences in the argument of Eq. (4) are determined only by the electron energy $2E_P' + E_C$ at the initial Fe_{Li}^{2+} ion (Appendix A). The best fit[17] to the low energy onset of the absorption band (Fig. 2), up to the band peak at 2.6 eV, is obtained with $E_P' = 0.70$ eV and $E_C = 1.22$ eV, assuming $\hbar\omega_0 = 0.1$ eV. The energy E_C should not be interpreted as the energy distance of the $Fe_{Li}^{2+/3+}$ level below the rigid lattice conduction band; for details, see Appendix B.

How does the arrangement of the final site Nb ions (Fig. 1) determine the relative intensities and the polarizations of the contributing individual transitions? Each of the contributions in Eq. (4) depends on the products $d_i^2 J_i^2$. The integral J_i

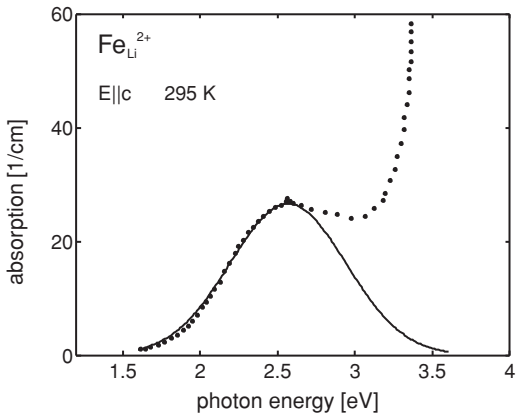

FIG. 2. Optical absorption of Fe^{2+}_{Li} in LN. The experimental data (dots) are reproduced (Ref. 17) (full line) at energies up to the peak near 2.6 eV by the small polaron approach [Eq. (4)]. The deviation between this small polaron prediction and experiment at energies higher than the peak energy is attributed (Ref. 17) to excitations to extended states lying within the conduction band. In this range, there is also a superposition with transitions from the valence to the conduction band, rising steeply. We note that a small peak is superimposed on the broad band; it is caused by Fe^{3+} spin forbidden transitions (Ref. 20).

typically decreases with rising d_i in an exponential way. This decrease dominates the product $d_i^2 J_i^2$ at larger distances. For a simple two-center molecule, e.g., H_2^+, the maximum of $d^2 J^2(d)$ occurs at about 70% of the bond length.[38]

As indicated in Fig. 1(b), there are three equivalent Nb ions in the plane perpendicular to c [i.e., Nb(1), Nb(2), and Nb(3)], which are lying above Fe, and three further ones [Nb(4), Nb(5), and Nb(6)] below Fe. The Fe-Nb bonds d_1, d_2, and d_3 all enclose an angle of 77° with c [Fig. 1(a)]. For the second set of Nb ions (d_4, d_5, and d_6), the angle is 61°. Since these latter bonds are considerably longer [Fig. 1(a)] than the former ones, they contribute less to the total absorption. Among the bonds extending along the c axis, d_7 is shorter than d_8 and thus leads to a stronger absorption. Only the bonds d_1 to d_6 have projections perpendicular to c, and therefore only transitions along these bonds are caused by ordinarily polarized light. Their projections on the c axis are rather small and, thus, the absorption by extraordinarily polarized light is dominated by transitions along d_7.

On this basis, it can be understood why the superposition of the transitions along the directions d_1 to d_8 will cause that the Fe-Nb transfer band at 2.6 eV is only slightly polarized. In fact, experiment shows that the absorption is almost isotropic, with the ordinary one being more intense by about 10% than the extraordinary one.[35]

It must be noticed, however, that the J_i integrals do not only depend on distance d_i: The arrangement [Fig. 1(a)] of the orbitals $|I\rangle$ and $|F_1\rangle$ as well as $|F_7\rangle$, being examples for nonaxial and axial Fe-Nb neighbors, show that also the relative orbital orientations will determine the magnitude of the J_i. Furthermore, the positions of the intercalated O^{2-} ions, forming indirect bonds, will have to be taken into account for the size of the J_i. Therefore, taking into account only the distance dependence of $d_i^2 J_i^2$ as the sole influence on the intensities must be considered to be only an approximate approach. Both these contributions will also cause that the polarizations of the transitions are only approximately directed along the bond directions d_i.

C. On the relative sizes of the elements of the photovoltaic tensor

This section will treat the light-induced changes of the Fe-Nb dipoles as the initial steps of the photovoltaic current. Since these excitations will trigger all the subsequent processes, such as the coherent band transport as well as the following incoherent hopping charge movements (both treated in Sec. III), the tensor description, to be outlined here, will govern the complete sequence of the events contributing to the photovoltaic phenomena.

First, we return to the optical absorption, which can be described, following Eq. (A5) of Appendix A, in this way:

$$\alpha_{\text{tot}} = \sum_i \alpha_i \propto \sum_{i=1,\ldots,8} \langle I'|r_l|F_i'\rangle\langle F_i'|r_k|I'\rangle \cdot e_l e_k^* \cdot I. \tag{5}$$

Here, the matrix elements $\langle I'|r_l|F_i'\rangle$ and $\langle F_i'|r_k|I'\rangle$ represent the values expected for the respective transition dipole arms r_l and r_k; they are multiplied with the related components e_l and e_k^* of the unit vectors along the photon electric fields.

Each of the eight terms in the sum [Eq. (5)] is proportional to the transition probability to one of the eight Nb^{5+}_{Nb} neighbors and thus represents a time-dependent change of the related Fe^{2+}_{Li}-Nb^{5+}_{Nb} dipole, i.e., a local current. We specialize first on the most important situation that the net electronic current $\mathbf{j}$ flows along the c direction, $\mathbf{j} \parallel c$. All transitions to the Nb ions lying above Fe in Fig. 1(a), i.e., Nb(1), Nb(2), Nb(3), and Nb(7), have positive projections on the $+c$ direction, and those lying below Fe, i.e., Nb(4), Nb(5), Nb(6), and Nb(8), have negative ones. With the appropriate modification of Eq. (5), one arrives at

$$j_z \propto \left\{ \sum_{1,2,3,7} \langle I'|r_k|F_i'\rangle\langle F_i'|r_l|I'\rangle - \sum_{4,5,6,8} \langle I'|r_k|F_i'\rangle\langle F_i'|r_l|I'\rangle \right\} \times e_k e_l^* \cdot I = j_+ - j_-. \tag{6}$$

Equation (6) indicates that the first and the second sums are related to the current along the positive and the negative directions of the c axis, respectively. The analogy of Eq. (6) to the phenomenological description $j_i = \beta_{ikl} e_k e_l^* \cdot I$ [Eq. (1)] is obvious and allows us to interpret the experimentally determined values of the β_{ikl} within the intervalence transfer model, as sketched in the following. We shall first continue to treat currents parallel to c, i.e., j_z, and will deal with currents perpendicular to c, i.e., j_y, below. The structure of Eq. (6) is similar to that of Eq. (5), except for the following distinctions: (1) Differences of dipole changes along the positive and negative c axis have to be considered instead of their sums. (2) These dipole changes now have to be projected on the c axis in order to lead to j_z. Figure 1(a) shows that extraordinarily polarized light will essentially only activate transitions along the bonds d_7 and d_8. Dipole changes along d_7 will dominate those along d_8 because the former distance is shorter, yielding larger values of $d_i^2 J_i^2$. This comparison of distances is justified

since the orbitals at Nb(7), Nb(8), and at Fe_{Li}, all extending along this axis, have the same relative orientations.

A situation decisively different from that related to the j_z case [Fig. 1(a)] is met for j_y [Fig. 1(b)]. Here, the projections of all Fe-Nb distances on the plane perpendicular to c are equal. The currents $j \perp c$ can thus not be attributed to the differences of the distances d_i. In this $j \perp c$ case, net currents can arise because now the comparatively minor dependence of the J_i^2 on the coupling between Fe^{2+} and Nb^{5+} ions, mediated by the intercalated O^{2-} ions, is decisive. They form Fe-O-Nb indirect bonds [Fig. 1(b)], comprising bond distances of varying lengths. The shorter the bonds [see Fig. 1(b)], the higher the contribution they make to the indirect coupling. It is seen on this basis that, for instance, the current along $+y$, i.e., from the Fe_{Li}^{2+} in the center of Fig. 1(b) to the right $Nb^{5+}(1)$ (connected by two O^{2-} ions along the distance sequences 1.89/2.24 Å, 2.07/2.11 Å) is stronger than along $-y$, to the left one, Nb(4), where there is essentially only one intercalated O^{2-} ion (distance sequence 2.07/1.89 Å); the second path contains the very long O^{2-}-Nb(4) distance of 3.75 Å, and hence a weak coupling can be expected. Because of these unequal bonding conditions along $+y$ and $-y$, a net current can arise along the y direction as well.

It has not been considered so far that the light-induced transfer of an electron also triggers the displacement of ions when they adjust to the new position of the transferred electron. Also, these ionic movements represent currents and contribute to the total photovoltaic effect. Since they are kicked off by the fast initial electronic transitions, the description by the tensor elements in Eq. (9) also comprises such currents and all the following further ionic and electronic charge displacements to be discussed below. Empirical data for the ionic movements following the ionization of Fe_{Li}^{2+} are not available. For the analogous case of the Nb_{Li}^{4+} antisite defect, Nahm and Park[39] report that removal of the electron shifts the ion by 0.04 Å (about 1% of the bond length) along the negative c axis. Similar effects are expected to occur as the consequence of the ionization of Fe_{Li}^{2+}. Such a downward movement of the ionized ion supports the experimentally established negative charging of the $+c$ end of the crystal by electronic transfer. Because of the related small displacements, such photoinduced ionic currents can safely be neglected in comparison with the much longer electronic transfer lengths (see Sec. III).

So far, the phenomena leading to the coherent photovoltaic currents, which result from the light-induced absorption by Fe_{Li}^{2+} in congruently melting LN, have been discussed. These properties are essentially identical to those observed with LN:Fe with changed Li/Nb ratios or doped additionally with Mg.[40] Apparently, it is only the initial transfer from Fe_{Li}^{2+} to neighboring Nb_{Nb}^{5+} conduction states that is responsible for the current. As will be discussed below, the intrinsic or extrinsic defects present at more distant sites in the crystal will influence the conductivity determined by the incoherent part of the conduction.

D. On the photovoltaic activity of defects on Li sites

In Sec II C, we deduced why the elements of the photovoltaic tensor related to $j \parallel c$ are much larger than those pertaining to $j \perp c$. This results from the special geometry of the structural environment of the Fe_{Li} site in LN where the Fe^{2+} ion is incorporated, which is characterized by a strong asymmetry of the projections of the responsible bond lengths on the c axis. We further remark that the initial currents do not depend directly on the energy difference between the electron at its initial site Fe_{Li}^{2+} and at its final positions Nb_{Nb}^{4+}. It is only the light-induced changes of the corresponding dipole moments that form the current.

It is thus expected that also alternative defects, intrinsic as well as extrinsic ones, located at Li sites in LN will lead to comparable photovoltaic effects. Therefore, it is not surprising that, for instance, optical absorption by a small polaron bound to the Nb_{Li}^{5+} antisite defect causes photovoltaic currents.[41] The orbital topology of this defect is identical to that of Fe_{Li}^{2+}.[17,39] Since the defect potential of Nb_{Li}^{4+} is smaller ($E_C = 0.53$ eV, $E_P' = 0.58$ eV) than that of Fe_{Li}^{2+} ($E_C = 1.22$ eV, $E_P' = 0.70$ eV),[17] the transfer mixture between initial $|I\rangle$ and final $|F\rangle$ orbitals is less asymmetric [the diagonal element in Eq. (A2) becomes smaller relative to the off-diagonal J], and the coupling of the initial to the final Nb_{Nb}^{5+} orbital by J_i is more decisive. On this basis, it can be understood why the transfer absorption cross section of Nb_{Li}^{4+} is stronger than that of Fe_{Li}^{2+}. Merschjann *et al.*[42] report the maximal cross sections $(7 \pm 2) \times 10^{-22}$ m^2 for Nb_{Li} and $(4.5 \pm 0.8) \times 10^{-22}$ m^2 for Fe_{Li}^{2+} at 785 and 488 nm, respectively. This supports the increase of the photorefractivity in LN, mainly determined by the BPVE,[2,3] if the Nb_{Li}^{4+} charge state is populated.[43] In passing, we note that the absorption cross section of the Nb_{Li}^{4+}-Nb_{Nb}^{4+} bipolarons is about twice as large, $(14 \pm 2) \times 10^{-22}$ m^2, than that of Nb_{Li}^{4+}[42]; the two electrons in the bipolaron ground state[17] cause a doubling of the oscillator strength, in line with the sum rule for oscillator strengths. Bipolarons in LN are therefore likely to lead to stronger photovoltaic currents. Also, optical absorption by further extrinsic defects, known to be incorporated on Li sites[44] such as Cu^{2+}, Ni^{2+}, Co^{2+}, and Mn^{2+}, are known to cause BPV currents.[45] Defects on regular Nb_{Nb} sites, on the other hand, are not expected to be active in this respect because the bonds to their 12 nearest Nb_{Nb}^{5+} neighbors have equal projections along the positive as well as the negative c axis.

III. SHORT-CIRCUIT PHOTOVOLTAIC CURRENT AND OPEN-CIRCUIT VOLTAGE

A. Some defining remarks

When treating now the further aspects of the BPVE, we have to consider that the initial light-induced change of the ith Fe_{Li}-Nb_{Nb} dipole represents the first step of a corresponding current j_i carried by band states extending further into the crystal. This current is transported in a coherent way, as j_{coh}, keeping its directional properties before being randomized by interaction with the lattice. Measurements of the Hall effect of the photovoltaic current[46,47] have proven this in a clear way; this coherent current corresponds to a ballistic motion before relaxation of the initial momentum. It has to be investigated how this current turns over into an incoherent one, j_{incoh}, representing thermally activated hopping transport in the present situation. The interrelation of both types of currents has been treated theoretically in detail by Heyszenau,[16] showing

that it is eventually the incoherent part, which is measured at the ends of the crystal. We shall show how the present small-polaron-related facts fill this general framework.

It is the sum over all individual coherent currents j_i ($i = 1, \ldots, 8$) that leads to the total photovoltaic current. Concentrating again only on the $j \parallel c$ case, these local currents contribute only by their projection on the c axis. The resulting $j_{i,z}$ are weighted by the related transition probabilities p_i; this leads to the total initial current j_{coh} along the c axis. By each of the components j_i, the electron is displaced by a projected transport length $l_{i,z}^{\mathrm{coh}}$. Because the light-induced dipole changes depend on the index i, also the related transport lengths are indexed by i. The mean transport length $\Lambda_z^{\mathrm{coh}}(\hbar\omega)$ along the c axis is then

$$\Lambda_z^{\mathrm{coh}}(\hbar\omega) = \frac{\sum_{1,2,3,7} p_i(\hbar\omega) l_{i,z}^{\mathrm{coh}} - \sum_{4,5,6,8} p_i(\hbar\omega) l_{i,z}^{\mathrm{coh}}}{\sum_{i=1,\ldots,8} p_i(\hbar\omega)}. \quad (7)$$

The superscripts coh, here attached to $l_{i,z}$ and Λ_z for clarity, will not be used any more in the following.

In the small polaron approach, the transition probabilities p_i are given by Eq. (4):

$$p_i(\hbar\omega) \sim d_i^2 J_i^2/\omega \exp[-w(\hbar\omega - 2E_P^{'} - E_C)^2]. \quad (8)$$

The ω dependencies contained in Eq. (8) do not influence $\Lambda_z(\hbar\omega)$ [Eq. (7)] because the ω related factors in Eq. (8) are identical for all transitions i. The indicated dependence of Λ_z on $\hbar\omega$ expresses the fact that the $l_{i,z}$ depend on photon energy. After optical absorption $\alpha(\hbar\omega)$ has transferred an electron within a $\mathrm{Fe_{Li}}$-$\mathrm{Nb_{Nb}}$ dipole to an unrelaxed state at the final site, it must be ionized from there in order to initiate the current j_{coh}, which is not randomized by scattering. The ionization probability or, equivalently, the quantum efficiency and the related coherent transport length $l_{i,z}$, are described by the Glass factor $\kappa(\hbar\omega)$.[1] These parameters are combined in the relation[1]

$$j_{\mathrm{coh}} = \alpha(\hbar\omega)\kappa(\hbar\omega)I. \quad (9)$$

Equation (9) is analogous to Eq. (1), simplified to a scalar by concentrating on the dominating current component $j \parallel c$. While all the information available for optical transfer transitions in centrosymmetric compounds is contained in the coefficient $\alpha(\hbar\omega)$, for noncentrosymmetric materials, the identification of $\kappa(\hbar\omega)$ is an extra bonus, which yields further information on the initial propagation of the electron photoionized from $\mathrm{Fe_{Li}^{2+}}$ up to its first scattering event.

B. Formation of the coherent current and energy dependence of the Glass factor

In Fig. 3, the energy dependence of $\kappa(\hbar\omega)$ (Refs. 1 and 48) is compared with that of $\alpha(\hbar\omega)$. It is seen that the peak energy of $\kappa(\hbar\omega)$ at about 3.1 eV is higher than that of $\alpha(\hbar\omega)$ at 2.6 eV. It should be noted also that the photon energy dependence of the Hall effect of the photovoltaic current is peaked at the same energy and has the same shape as $\kappa(\hbar\omega)$.[49] According to the interpretation of this Hall effect,[47] the physics of $\kappa(\hbar\omega)$ must therefore be determined by the initial coherent, ballistically moving current, as mentioned before. The increase of $\kappa(\hbar\omega)$ with photon energy, different from $\alpha(\hbar\omega)$, thus has to be attributed to a rise of the coherent transport lengths and/or the ionization probability. As noted previously,[17] the interpretation

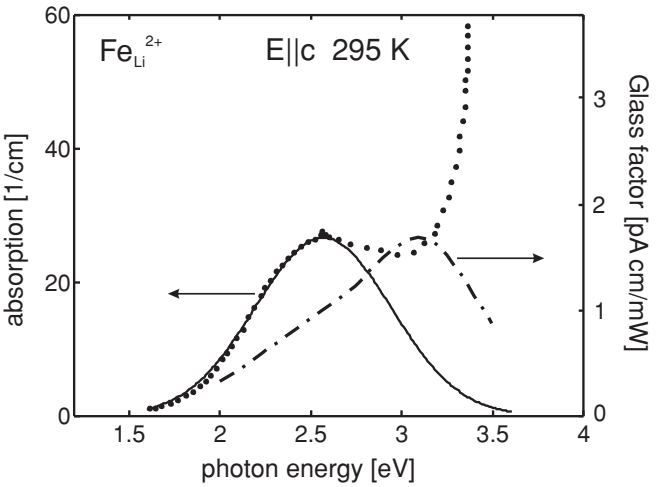

FIG. 3. Comparison of the energy dependences of the absorption $\alpha(\hbar\omega)$ (Ref. 17) and the Glass factor $\kappa(\hbar\omega)$ (Ref. 48) for LN:$\mathrm{Fe_{Li}^{2+}}$. The maximum of $\kappa(\hbar\omega)$, about 3.1 eV, lies at energies where α is likely to be attributed to optical excitations to delocalized final states (Ref. 17). This suggests that ionization into such bandlike states is at the root of the BPVE as discussed in the text.

of the absorption shape $\alpha(\hbar\omega)$ suggests that electrons excited to energies above its peak energy (2.6 eV) are delocalized over several $\mathrm{Nb_{Nb}}$ sites. This observation initiates a chain of arguments, to be presented in the following, explaining why the ionization probability as well as the transport lengths, both contributing to $\kappa(\hbar\omega)$, are expected to increase with rising photon energy.

As stated before, it is a necessary condition for the formation of a BPV current that a fraction of the electrons optically transferred to $\mathrm{Nb_{Nb}^{5+}}$ (Fig. 1) do not return to their initial $\mathrm{Fe_{Li}^{3+}}$ sites. Each backward step of this type would completely compensate the corresponding light-induced forward current, which is composed of electronic as well as ionic contributions. Ideally, the quantum efficiency for the separation of the carrier from the $\mathrm{Nb_{Nb}^{4+}}$ site, reached by optical excitation, should be as close to unity as possible. In this case, all optically excited electrons would contribute to the short-circuit photovoltaic current. In the opposite case, optical rectification,[12] represented by the transient changes of the Fe-Nb dipoles, would prevail, with all net dipoles being aligned along the same direction in the ferroelectric LN. Such transient dipoles exist only until the electrons have returned from $\mathrm{Nb^{4+}}$ to their initial $\mathrm{Fe^{3+}}$ sites and, thus, do not yield a steady current.

How does the separation of the electron from $\mathrm{Nb_{Nb}^{4+}}$ proceed? At first, such a process appears to be unlikely because a recombination of the electron back to $\mathrm{Fe_{Li}^{3+}}$ is supported by the local electric field formed by the excitation, attracting the electron to the empty $\mathrm{Fe_{Li}^{3+}}$. Furthermore, as sketched in Fig. 4, there is no barrier (see Appendix B) for this decay along the visited potential sheets, allowing a direct return by multiphonon emission without the need for intermediate thermal excitation. Such a relaxation process is expected to occur on a subpicosecond time scale. In addition, also the photovoltaic (PV) macroscopic electric field, developing across the end faces of the crystal under the flow of the PV

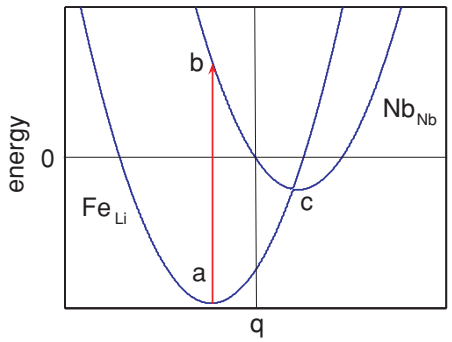

FIG. 4. (Color online) Scheme of the Fe-Nb potential sheets, allowing us to indicate the small polaron optical excitation from Fe_{Li}^{2+} to Nb_{Nb}^{5+}. $a \rightarrow b$: Here the electron is moved forward to a potential sheet centered around Nb_{Nb}^{5+}, while the lattice is fixed. $b \rightarrow c$: The Franck-Condon excited lattice adapts to the new electronic state Nb_{Nb}^{4+}, accompanied by multiphonon emission. At c, the electron crosses to the potential sheet centered around Fe_{Li}^{3+} (backward movement). $c \rightarrow a$: The lattice adapts to the newly formed Fe_{Li}^{2+}, again emitting many phonons. For the derivation of this scheme, see Appendix B.

current (see below), if not short circuited, tends to drive the electron back to its home site Fe_{Li}^{3+}.

Among the mechanisms impeding backward recombination is the fast relaxation of the forward moving j_{coh} to j_{incoh}, to be discussed below. The comparatively low mobility of j_{incoh} will hinder the backward flow. Furthermore, there is a certain probability that the Franck-Condon excited electron, having energies resonant with the conduction band (Fig. 5),

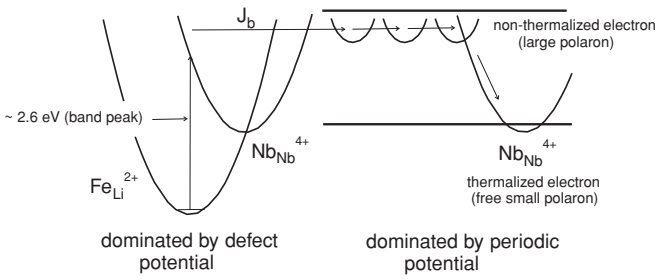

FIG. 5. Scheme of the Franck-Condon intervalence transitions from Fe_{Li}^{2+} to Nb_{Nb}^{5+} final states and of the processes following this initial step. At low photon energies, the transitions are dominated by the local Fe_{Li} defect potential, and hybridization with the conduction band states is then low. Ionization from such low-lying initial excited states is weak and the Glass factor $\kappa(\hbar\omega)$ is accordingly small (Fig. 4). At higher energies, the localizing influence of the defect is less decisive; ionization, mediated by a transfer integral J_b, and tunneling farther into the crystal is more pronounced and the Glass factor is thus expected to rise continuously with photon energy. It is presumed that the coherent tunneling movement occurs in the form of large polarons; the coupling to the lattice accompanying the extended electronic tunneling is symbolized by truncated parabolae. In such optically excited states, the carriers are not thermalized. They can lose their surplus energy by forming free Nb_{Nb}^{4+} small polarons having ground state energies slightly below the rigid lattice conduction band continuum. From there, the polarons can be transferred, by thermally activated hopping, to lower defect states, provided, for instance, by Nb_{Li} defects and further Fe_{Li} ions.

tunnels away from the initial Nb_{Nb} site reached after optical transfer. Optical excitations will occupy such bandlike states if the transfer integrals connecting also with Nb_{Nb}^{5+} ions farther removed into the crystal are sizable enough. Also, such transfers exceeding the first Nb_{Nb} coordination sphere around Fe_{Li} will form part of the coherent current j_{coh} as long as their directed movement is not statistically randomized with respect to the transfer direction.

At low photon energies, the final state reached by the excitation is expected to be dominated by the influence of the local Fe_{Li} defect potential (Fig. 5), whereas for higher energies, coupling to the extended bandlike states prevails. The actual mixture between local and extended states is rather involved. This is demonstrated for the analogous case of an electron captured as a small polaron at a Nb_{Li}^{5+} antisite defect: Nahm and Park[39] have calculated the related excited energy levels lying in the conduction band continuum, all projected into a unit cell in **k** space, resulting from the combined influence of bandlike tunneling, the defect potential, and the polaron-type lattice distortions. Since the evolving scheme of the related levels, lying in the range of the conduction band, is rather complex and, since corresponding data are not available for the excited states of the Fe_{Li} defect, we derive an estimate for an upper bound of the distance that an electron can tunnel away from Nb_{Nb}^{4+} after the initial excitation. It is assumed that the electron is excited at high photon energies into the fully developed band. The electron first forms a wave packet around the final site Nb_{Nb}^{4+} ion, which is coupled by a transfer integral J_b, essentially the one describing the formation of the conduction band to its equivalent Nb_{Nb}^{5+} neighbors. With this quantity, the quantum diffusion, resembling coherent band motion, will cover a mean distance of $x = c\sqrt{(J_b\tau/\hbar)}$ ($J_b/\hbar$: rate of site change by quantum diffusion, corresponding to band transport; c: Nb_{Nb}-Nb_{Nb} distance along the c axis, 6.9 Å). Here $\tau \sim 10^{-13}$ s, the mean time needed for relaxation to the Nb_{Nb}^{4+} free polaron ground state,[18,19] and $J_b \sim 0.7$ eV, as taken from the full width $2J_b$ of the lowest conduction band of LN determined from a rigid lattice calculation to be ≈1.5 eV.[50] Thus, $x \sim 3.3c = 23$ Å, indicating that the electron moves at most several Nb_{Nb}-Nb_{Nb} distances coherently along the c axis before the lattice relaxes around it to form a Nb_{Nb}^{4+} small polaron ground state (Fig. 5); this terminates the coherent transport. From this estimate for the individually covered distance l_i, one arrives at the mean distance Λ_z, according to Eq. (7), by projecting l_i on the c axis and then averaging the resulting $l_{i,z}$ over all eight transfer paths. Therefore, even the upper limit of Λ_z can be much shorter than the estimated l_i.

This given upper limit for l_i is based on the assumption that the electron was excited into the range of the fully developed band. The J_b integrals corresponding to the unperturbed band[50] were used. For lower energies, the influences of the local defect potential and the localizing polaron distortion will impede the separation from the initial site, and the coherent movement away from Nb_{Nb}^{4+} next to Fe_{Li} will be smaller. Since both influences, ionization as well as subsequent tunneling transport length, depend on the photon energy, this can explain the energy dependence of $\kappa(\hbar\omega)$ qualitatively (Fig. 5).

The continuous change of the nature of the final states in the intervalence transition with rising energy can be seen from the energy dependence of the optical absorption (Fig. 2).

Up to the peak energy ~2.6 eV, the absorption can be reproduced by the typical small polaron approach (Appendix A), implying that the excited state tends to be localized by coupling to the lattice. The deviation between experiment and theory at higher energies was attributed[17] to an increasing tunneling delocalization, i.e., an onset of banding. The same type of energy dependence of $\alpha(\hbar\omega)$, pointing to delocalization when the photon energy rises above the lower conduction band edge, was also observed for the Nb_{Li} antisite defect and the Nb_{Li}-Nb_{Nb} bipolarons.[17] All these turn out to be special examples for the optical absorption of small polarons, in general, where the optical absorption at higher energies is usually larger than predicted by conventional small polaron theory. There, the tendency of delocalization at elevated Franck-Condon energies lying in the band regime is neglected (see, e.g., Ref. 51).

Beyond the peak energy of the Glass factor $\kappa(\hbar\omega)$, the absorption starts to be dominated by transitions from the valence band, essentially of O^{2-} character, to the Nb_{Nb}^{4+}-type conduction band. Possibly, such transitions are less decisive in creating a BPVE than defect conduction band excitations.

The formation of coherent tunneling states among several equivalent sites after Franck-Condon excitation from an initial small polaron ground state into final states resonant with a band has been proven by experiments with very well-characterized model systems, O^- hole small polarons in oxide materials.[52] Here, the holes are bound to (negatively charged) acceptor cores and the symmetry of the systems is thus pointlike. A hole is localized at just one of the O^{2-} ions around the acceptor core. This is caused by lattice distortion, and the hole thus forms a small polaron bound to the acceptor. Optical excitations occur from the initial O^- site to one of the equivalent O^{2-} neighbors. Because of the nature of the Franck-Condon transitions, the excited final hole states are lying within the valence band. Although there is a strong coupling to the lattice at each of these excited oxygen sites visited by the hole, the lifetime of the excited carrier is long enough that stationary tunneling states form before the lattice relaxes to the formation of the polaron at another O^{2-} site. The existence of such extended coherent states in the presence of even strong coupling to the lattice is characteristic for a large polaron; here it is realized by the optically excited states.

This example leads to the expectation that, in the present translational symmetry (all Nb_{Nb} ions of the lattice are equivalent), an optically excited large polaron state extends through the crystal. Depending on the energy-dependent overlap of the electron excited to a first Nb_{Nb} site with these large polaron states, there will be a corresponding tendency to tunnel away into the crystal.

A direct experimental proof for the strong energy-dependent increase of the ionization probability of a defect having electronic density mainly at a Nb_{Li} site is available from electron paramagnetic resonance (EPR) studies[53,54] of the light-induced dissociation of Nb_{Li}^{4+}-Nb_{Nb}^{4+} bipolarons. Here, both electrons captured in this molecule tend to be near the Nb_{Li} site.[39] This dissociation reflects the optical transfer of bipolaron electrons to energy levels within the conduction band. The influences of the defect potential and the surrounding polaronic displacements, both tending to localize the carrier, decrease with rising photon energy.[17]

As discussed for the present case, LN:Fe, the coherent bandlike initial movement of an electron along the positive c axis is characterized by a mean directed coherent transport distance $\Lambda_z(\hbar\omega)$ [Eq. (7)] increasing with rising photon energy. Such transport processes are terminated by ionic displacements around the electron, forming a Nb_{Nb}^{4+} free small polaron, which is representative for the ground state of the LN conduction band in the real, not rigid, LN crystal. The formation of the Nb_{Nb}^{4+} polarons from optically created nonthermalized electrons has been proven experimentally by Qiu *et al.*[18] and by Sasamoto *et al.*[19] By using a pump-probe setup with a temporal resolution below 0.1 ps, these authors monitored the rise of the Nb_{Nb}^{4+} free small polaron optical absorption[55] and found that it occurs after about 10^{-13} s at room temperature.

So far, the phenomena leading to the coherent photovoltaic currents, which result from the light-induced absorption by Fe_{Li}^{2+} in congruently melting LN, have been discussed. These properties are essentially identical to those observed with LN:Fe with changed Li/Nb ratios or doped additionally with Mg.[40] Apparently, it is only the initial transfer from Fe_{Li}^{2+} to neighboring Nb_{Nb}^{5+} conduction states that is responsible for the current. As will be discussed below, the intrinsic or extrinsic defects present at more distant sites in the crystal, introduced by changing the Li/Nb ratio or by doping with Mg, will influence the (photo)conductivity determined by the incoherent part of the conduction.

C. Turnover to the incoherent current

It is, thus, concluded that optical excitation of electrons to band states almost immediately (within $\sim 10^{-13}$ s) leads to the occupation of states near the lower edge of the conduction band, where the carriers are represented by free Nb_{Nb}^{4+} small polarons in the real, not rigid, lattice. Their formation from the coherently transported nonthermal carriers represents the initial step toward incoherent motion, leading to j_{incoh}, since small polarons are characterized by hopping-type diffusive site changes. For the Nb_{Nb}^{4+} conduction polarons, the related activation energy is 0.27 eV.[17] During their diffusion, they can also be trapped at defects having lower-lying levels, such as Nb_{Li}^{5+} antisite defects present at 1% of all Li sites in congruently melting LN (CLN), or at one of the further Fe_{Li}^{3+} impurities, usually present with lower concentrations. These steps form a cascade of events ordered by characteristic time spans.[56,57]

Since diffusion by itself, described by a second-rank tensor, distinguishes a special direction only in the presence of a concentration gradient (not caused by the homogeneous illumination under which the BPVE is studied), the question arises as to how the initial coherent movement transfers its characteristic average direction to the diffusive transport in such a way that a continuous directed current throughout the crystal arises. Our argument is based on Fig. 6(a), adapted from Ref. 16. Under optical excitation, an electron can be transferred from Fe_{Li}^{2+}, point I in Fig. 6, into the band state, as discussed initially above, where it is transported as j_{coh} along the distance $\Lambda_z(\hbar\omega)$ up to point II. At this termination of the coherent motion by formation of a free Nb_{Nb}^{4+} small polaron, it contributes again to the diffusive current. Here, retrapping at the deeper defects, such as Nb_{Li}^{5+} and Fe_{Li}^{3+}, takes place

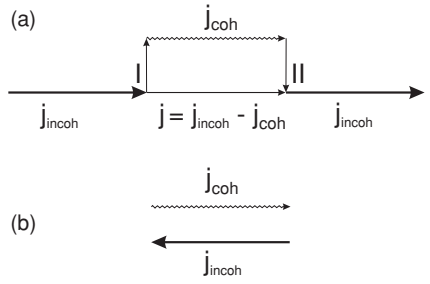

FIG. 6. (a) Short-circuit situation, supporting the discussion (see text) of the direction of the incoherent, diffusive current as related to the coherent one. For details, see text. (b) Open-circuit situation: the coherent forward current is compensated to zero by the incoherent backward drift current, driven by the open-circuit field $E_{\rm phv}$. Also, in this case of a zero net current, a photovoltaic Hall effect is measured (Ref. 46): essentially, only the coherent part contributes to it because of the very low mobility of the incoherent part.

eventually. Since the diffusive currents are undirected in the absence of a concentration gradient, it is not *a priori* clear why they should be directed as indicated in Fig. 6. Because, however, $j_{\rm coh}$ is in most cases directed along $+c$ (here we restrict always our attention to this most important case), continuity requires that also the complete diffusive current $j_{\rm incoh}$, which is eventually measured as the BPV current, is directed along c. For an extended analytic treatment of these events, we refer to the related elaboration by Heyszenau.[16]

It is, thus, the coherent bandlike transport along $\Lambda_z(\hbar\omega)$ that triggers the directed net current $j_{\rm phv}$, written as a scalar, throughout the crystal. It is given by

$$j_{\rm phv} = e\dot{n}_e\Lambda_z(\hbar\omega). \tag{10}$$

Here, $\dot{n}_e$ is the optical production rate (concentration per unit time) of conducting electrons $\dot{n}_e = \alpha I\Phi/\hbar\omega$, proportional to the quantum efficiency Φ.

The mechanism of the creation of $j_{\rm phv}$, outlined above, indicates that this current is impressed into the crystal. Under open-circuit conditions, the end faces of the specimen can then be charged arbitrarily strongly, limited only by a backward current determined by the internal conductivity $\sigma = \sigma_d + \sigma_I$ (σ_d dark conductivity, σ_I photoconductivity). The open-circuit photovoltaic field is thus $E_{\rm phv} = j_{\rm phv}/\sigma$. Under this field, the backward current $j_{\rm back} = E_{\rm phv}\sigma$ compensates the forward, the photovoltaic current $j_{\rm phv}$ [Fig. 6(b)]. Written vectorially, therefore, $\mathbf{j}_{\rm phv}\mathbf{E}_{\rm phv} < 0$ as required for a source of electrical power. Also, the photoconductivity is determined by the optically generated incoherently diffusing electrons. Under high light intensities, $E_{\rm phv}$ is independent of the intensity since then both $j_{\rm phv}$ and σ_I are proportional to I ($\sigma_I \gg \sigma_d$).

As outlined, after illumination and formation of the Nb_{Nb}^{4+} free small conduction polarons, the measured photocurrent is essentially transported by such carriers. They contribute to the photoconductivity during their lifetime τ, i.e., as long as they are not trapped by deeper defects, where they are essentially immobile. Using μ for the mobility of the incoherently transported electrons in the following, when not stated differently, the photoconductivity σ_I is thus

$$\sigma_I = e\dot{n}_e\mu\tau \tag{11}$$

and, accordingly, the open-circuit field $j_{\rm phv}/\sigma_I$ is

$$E_{\rm phv} = \Lambda_z(\hbar\omega)/\mu\tau. \tag{12}$$

With congruently melting LN, $E_{\rm phv} \sim 10^5$ V/cm has been measured.[1] The mean transport length $\Lambda_z(\hbar\omega)$ has been determined to be about 1 Å.[1] This implies that $\mu\tau \sim 10^{-13}$ $\rm cm^2/V$ must be accounted for. The thermal hopping mobility of small polarons is given by $\mu = \mu_0\exp(-E_P/2k_BT)$ with $E_P/2 = 0.27$ eV for the conduction polarons in LN.[17] The prefactor $\mu_0 = eD_o/k_BT$ can be obtained from estimating the diffusion parameter $D_0 = a^2\nu$, where the Nb_{Nb}-Nb_{Nb} distance along the c axis, ~ 6.9 Å, is an estimate for the effective jump distance and ν is the hopping attempt frequency. By relating it to the assumed representative phonon energy $\hbar\omega_0 = 0.1$ eV, ν is determined to be $2.7 * 10^{13}$ 1/s. For 300 K, this yields $\mu_0 \sim 5$ $\rm cm^2/Vs$. Also, for 300 K, $\exp(-E_P/2k_BT) = 2\times10^{-5}$. The mobility of the conduction polarons is thus predicted to be $\mu \sim 1\times10^{-4}$ $\rm cm^2/Vs$, i.e., a factor 10^{-4} smaller than the lower bound for conduction in a wider band $\mu \geqslant 1$ $\rm cm^2/Vs$, often assumed.[58] The recombination time τ must be $\tau \sim 10^{-9}$ s in order to lead to $\mu\tau \sim 10^{-13}$ $\rm cm^2/V$.

The estimated mobility can be taken as an upper bound for the actual one because it is expected that, not only hopping between nearest Nb_{Nb} neighbors along the c axis, distance 6.9 Å, contribute to the diffusion, but also those lying at oblique angles with respect to this axis, which have shorter Nb-Nb distances. The actual mobility of the Nb_{Nb}^{4+} conduction polarons will thus be less than 10^{-4} $\rm cm^2/Vs$ and, thus, τ will be larger than 10^{-9} s.

The most detailed information on the lifetime τ in the Nb_{Nb}^{4+} conduction states is available for congruently melting LN, nominally undoped except for an addition of 5 mol% of MgO.[19] It is known that Mg is incorporated on Li sites, preventing the formation of Nb_{Li} antisite defects for the used MgO concentration. With such material, Sasamoto *et al.*[19] measured $\tau \sim 4\times10^{-8}$ s. Since the mean coherent electron displacement Λ_z is independent of the Mg doping,[40] also for Mg-doped material a recombination time τ somewhat larger than 10^{-9} s is expected. This is in accord with the experimental findings.[19]

For undoped congruently melting LN, it is expected that the lifetime τ is determined by trapping at the Nb_{Li}^{5+} antisite defects, present with a concentration of about 1% in such material. Accordingly, Sommerfeldt *et al.*[40] find a $\mu\tau$ product that is four times lower in these crystals than in those doped with 4.7% MgO; antisite defects are completely eliminated by this doping. This decrease of $\mu\tau$ by a factor of 4 is independent of the Fe^{3+} content of the respective specimens. Since the mobility μ is given by the polaronic properties of the Nb_{Nb}^{4+} electrons, it is the prolongation of the lifetime τ by Mg doping, eliminating the high concentration of Nb_{Li}^{5+} traps, that increases the photoconductivity, which is typical for strongly Mg-doped materials.

The direct experimental determination of the lifetime τ for undoped congruently melting LN so far presents some puzzles. While the pulsed pump-probe absorption measurements of LN:Mg (Ref. 19) show lifetimes completely independent of the polarization of the Nb_{Nb}^{4+} absorption band, the investigation of undoped LN shows a decay feature of the Nb_{Nb}^{4+} absorption only

for extraordinarily polarized pulses, leading to rather puzzling short lifetimes of 0.42 ps. Further experimental studies are required.

IV. DISCUSSION AND RELATION TO EARLIER WORK

Relying on recent insights into the polaronic features of the Fe_{Li}^{2+} defect in LN, the corresponding mechanism of the optical transfer to neighboring Nb_{Nb}^{5+} ions, the embedding of the resulting nonthermalized excited states into the conduction band structure of LN, the fast relaxation to free Nb_{Nb}^{4+} small conduction polarons, and on the subsequent trapping of such free polarons by deep defects, we could give a detailed and consistent explanation of the main characteristics of the BPVE in this material. The conclusion that the nonthermalized electrons are moving initially in a coherent, ballistic way, until this is ended by relaxation, is in line with results of earlier Hall-effect studies of the BPVE in the material.[46,47] The paramount roles of coupling of the electrons to the lattice and its competition with tunneling interactions were emphasized. There are essentially three items that require small polaron properties to account for the relevant observations: (1) The strong dependence of the transition probabilities on the Fe-Nb distances. This translates even rather small differences of such distances into a rather pronounced preferred transfer direction when averaged over all related transitions. (2) The strong increase of the Glass factor with rising photon energy is attributed in a straightforward way to the continuous transition from Franck-Condon excited local polaron states toward delocalized band states determined by the periodic potential of the crystal. (3) The firmly established conclusion that conduction carriers are free small polarons, having a very high thermal hopping activation energy, in a natural way accounts for the small mobility required to explain the exceptionally large open-circuit photovoltaic field E_{phv} of LN:Fe. The presented findings are expected to be further substantiated by detailed investigations by ultrafast absorption spectroscopy.

It has certainly become evident by now that the BPVE of LN:Fe is induced by optical transitions from the Fe_{Li}^{2+} defect to the conduction band. This is proved, e.g., by the coincidence of the energy thresholds of the optical absorption $\alpha(\hbar\omega)$ and of j_{phv} (Fig. 3), the latter represented by the Glass factor $\kappa(\hbar\omega)$. Alternatively, valence to conduction band transitions are conceivable causes for a BPVE (Ref. 11) if the created electrons and holes are bound by their Coulomb interaction or if simultaneously phonons are emitted and absorbed. In these cases, $j_{\mathrm{phv}}(\hbar\omega)$ should be strongest at energies close to the fundamental absorption, in contrast to the present situation.

In many aspects, the present modeling shows pronounced similarities to earlier proposals to explain the BPVE, especially in LN:Fe.[1,12,13,16,59] We shall now put these approaches into a perspective to the present elaboration.

Glass *et al.*,[1,12] immediately after realizing that the BPVE was a new phenomenon, attributed the sizable current along the c axis to the asymmetry of the Fe_{Li}-Nb_{Nb} distances with respect to the c axis, making them accountable for different probabilities for parallel and antiparallel transport p_+, p_-. Also, related different transport lengths l_+, l_- were introduced. On this basis, the authors derived an expression for the PV current, then only known to flow along the c axis:

$$j = j_+ - j_- = \alpha I \{(e/h\nu)(l_+ p_+ - l_- p_-)\}. \qquad (13)$$

This is equivalent to Eq. (6) and has similarities to Eq. (7) above. Comparing Eq. (13) with (9), it is seen that the expression in curly brackets has to be identified with κ. From measurements at 514 nm, Glass *et al.*[1] determined $\kappa = 3.0 \times 10^{-9}$ Acm/W and with 473 nm light, 4.8×10^{-9} Acm/W. Then, the mean transport length $(l_+ p_+ - l_- p_-)$ corresponds to 0.8 and 1.3 Å, respectively. In Sec. III B, an upper bound for an individual light induced transport length was estimated to be about 20 Å. Considering that Eq. (13) contains differences of such lengths and that, in p_+, p_-, also the ionization probabilities Φ (< 1) of Fe_{Li}^{2+} are included, there is consistency with the results for κ by Glass.[1] These authors also pointed out that ionic relaxation can contribute to the BPVE.[12] An internal efficiency (absorbed light power divided by electrical power) of 0.03% was reported.

In the absence of the more detailed experimental knowledge on the BPVE of LN:Fe available today, early theoretical attempts to explain the effect had to rely on general models, which were able to reproduce the main features known until then. Such approaches have been reported by Glass *et al.*[12] and von Baltz *et al.*,[13,14] as summarized by von Baltz[15] and by Ruppel *et al.*[60] As potentials hosting the intitial ground state, phenomenological structures were chosen, representing in the most simple and analytically accessible way the lacking inversion symmetry of the defect site. Optical excitations were considered to occur to simply structured final states lying in the conduction band. By appropriately choosing the phases of the final states, waves could be identified corresponding to transport in a definite direction. Also, a quadratic response theory was devised with consequences similar to those expressed by Eqs. (5) and (6), and the components of the photovoltaic tensor were derived in a formal way.

Heyszenau[16] presented more general considerations, pointing out that photoionization from an asymmetrically positioned defect, as in the present LN:Fe case, can cause a directed net current. As mentioned above, his work[16] also includes an extensive treatment under which conditions the electrons photoexcited from a defect can lead to a stationary photoinduced diffusive current correlated throughout an entire crystal and how this could account for the BPV current as well as the BPV field.

Belinicher and Sturman[29] and Sturman and Fridkin[11] presented a comprehensive study of the general principles governing the BPVE. These authors reported that a BPV current can also arise from band-band transitions induced by linearly polarized light if Coulomb interaction between electrons and holes prevails or, if, alternatively, phonon emission and absorption accompanies the optical absorption. For the special case of LN:Fe, treated by Sturman in 1991,[59] the main difference to the present interpretation is the value of the mobility μ responsible for the photoconductivity. Sturman *et al.*[58] claim that $\mu \sim 1$ $\mathrm{cm}^2/\mathrm{Vs}$. This value appears[59] to be inferred from the high Hall mobility $\mu^H = e\tau_{\mathrm{rel}}/m^* = 3 \times 10^3$ $\mathrm{cm}^2/\mathrm{Vs}$ (Refs. 46 and 47) of the BPV current, with m^* the bare (nonpolaronic) effective

band mass[46,47] and τ_{rel} the relaxation time terminating the initial coherent transport. From the measured μ^H, Levanyuk *et al.*[47] infer $\tau_{rel} \sim 10^{-13}$ s. This means that the initial ballistic transport is terminated within about the same, nowadays well-established,[18,19] time as the formation of the Nb_{Nb}^{4+} conduction polarons, having a mobility of $\sim 10^{-4}$ cm^2/Vs. There is, thus, not sufficient time that a local equilibrium among the nonthermal electrons can be established by multiple scattering. This would be the precondition for a diffusive transport, driven by a concentration gradient of the nonthermalized electrons, postulated by Sturman.[59] Since the BVPE can also be observed under homogeneous illumination, where no such conceivable concentration gradients can form, it can not be seen how a directed photovoltaic current can form by such diffusive transport of nonthermalized electrons.

It is stated sometimes (see, e.g., Ref. 61) that the BPV current in ferroelectric crystals is driven by the electric field caused by the polarization of such materials. Already, the observation that photovoltaic currents can also flow perpendicularly to the polarization axis argues against this model, extending the list of previous opposing arguments (see, e.g., Ref. 1).

ACKNOWLEDGMENT

The authors thank the Deutsche Forschungsgemeinschaft (DFG, Project No. IM 37/5-1) for financial support.

APPENDIX A: Fe_{Li}^{2+}-Nb_{Nb}^{5+} SMALL POLARON TRANSITIONS

Essential small polaron aspects in the present context are the dependencies of intensities on the transfer integrals J, on the frequency ω, and on the Fe_{Li}^{2+}-Nb_{Nb}^{5+} distance d.

The shape $\alpha(\omega)$ is determined by the distribution of probabilities $P(\omega)$ that photons of energy $\hbar\omega$ promote an electron from its initial energy at the Fe_{Li}^{2+} site to Nb_{Nb}^{5+}. We shall outline the related physics in a rather concise and therefore somewhat simplified way. At Fe_{Li}^{2+}, the electron is stabilized by the displacements of the surrounding ions, lowering its energy by $2E_P^{'}$ [$E_P^{'}$ total energy by small polaron formation, caused by the corresponding increase of lattice strain ($+E_P^{'}$) and lowering of the electronic energy ($-2E_P^{'}$)] and by the defect potential E_C. At the final Nb_{Nb}^{5+} site, there is no displacement related energy change as long as the electron is absent. Therefore, the mean electronic energy change accompanying the excitation of the electron under Franck-Condon conditions is $E = 2E_P^{'} + E_C$. For strong coupling, $E_P^{'} \gg \hbar\omega_0$ (representative phonon energy), of the electron to the lattice,[17,62] $P(\omega)$ is expressed by

$$P(\omega) \propto \exp[-w(\hbar\omega - 2E_P^{'} - E_C)^2] \tag{A1}$$

with $w^{-1} = \hbar\omega_0 4E_P^{'}$ (valid for $T = 0$, to be modified slightly for $T > 0$). The distribution $P(\omega)$ is continuous under the more realistic condition that not only phonons with $\hbar\omega_0$ but those with a dispersive spread of frequencies are coupled.

The dependence of the transition probability on the distance d can be derived by first treating the transfer admixture of the initial orbital $|I\rangle$ at Fe_{Li}^{2+} to that at the final site $|F\rangle$. Both are centered at sites having a distance d [Fig. 1(a)] from each other, mediated by a transfer integral J. This two-site mixture can be described by

$$H = \begin{pmatrix} -\Delta E & J \\ J & 0 \end{pmatrix} \tag{A2}$$

operating on the states $|I\rangle$ and $|F\rangle$. ΔE is the energy between the initial and the final sites, equal to the photon energy $\hbar\omega$. The transfer mixture leads to the first-order changes

$$|I'\rangle = |I\rangle + (J/\Delta E)|F\rangle \quad \text{and} \quad |F'\rangle = |F\rangle - (J/\Delta E)|I\rangle \tag{A3}$$

taking into account $J \ll \Delta E$, usually assumed for small polarons, and neglecting overlap corrections.

The dependence of the transition probability on the Fe_{Li}^{2+}-Nb_{Nb}^{5+} distance is inferred from the application of the Golden Rule formalism, yielding matrix elements related to the transition rates

$$M = \langle I'|\mathbf{r}\mathbf{E}(t)|F'\rangle\langle F'|\mathbf{r}\mathbf{E}(t)|I'\rangle. \tag{A4}$$

Here, $\mathbf{E}(t)$ is the light electric field and $\mathbf{r}$ is the transition dipole arm along the bond vector $\mathbf{d}$. This is, written in components,

$$\begin{aligned} M &= \langle I'|x_l|F'\rangle\langle F'|x_k|I'\rangle \cdot E_l(t)E_k^*(t) \\ &\propto \langle I'|x_l|F'\rangle\langle F'|x_k|I'\rangle \cdot e_l e_k^* \cdot I, \end{aligned} \tag{A5}$$

where summation over repeated indices is implied and the light intensity I is proportional to $E_l(t)E_k^*(t)$. The e_l and e_k are unit vectors along E_l and E_k. Because the orbitals $|I\rangle$ and $|F\rangle$ are centered around the Fe_{Li} and Nb_{Nb} sites, each of the matrix elements in Eq. (A5) is approximately

$$\langle x_l\rangle \approx (J/\hbar\omega)\, d_l. \tag{A6}$$

Since the transitions are accompanied by the absorption of a photon with energy $\hbar\omega$, the energy absorption rate, expressed by the optical absorption, is

$$\alpha(\omega) \propto J^2 d^2/\omega \exp[-w(\hbar\omega - 2E_{P'} - E_C)^2] \tag{A7}$$

yielding the dependence of the absorption on J, d, and ω. The powers with which they enter into Eq. (A7) agree with those resulting from the exact theory.[22,25–27]

APPENDIX B: Fe_{Li}^{2+}-Nb_{Nb}^{5+} SYSTEM AND Nb_{Nb}^{4+} FREE POLARONS

Some energies related to the Fe-Nb system are quoted in Figs. 4 and 5. The physical arguments leading to the shown potential schemes will now be pointed out. The optical as well as the thermal transitions from Fe to Nb can be visualized in a rather transparent way if both systems are treated within a common coordinate system, represented by the difference of the respective local ion displacements.[17]

We first focus our attention on two equivalent sites, e.g., two Nb_{Nb}^{5+} ions being part of the ideal LN crystal. This is related to the physics of free Nb_{Nb}^{4+} conduction small polarons. Upon capturing an electron at one Nb_{Nb}^{5+}, forming Nb_{Nb}^{4+}, the force exerted by this charge change will displace the neighboring ions, i.e., essentially O^{2-} ions; the resulting increase of the strain energy is labeled KQ^2, where a single interaction coordinate Q is used for brevity. This distortion also leads

to a lowering of the energy of the new electron at Nb_{Nb}^{4+}, described by the electronic energy $-VQ$ with the respective force constant V.

The total displacement dependent energy at sites 1 and 2 is

$$E_{\rm tot} = E_1 + E_2 = KQ_1^2 + KQ_2^2 - V(n_1Q_1 + n_2Q_2), \tag{B1}$$

where $n_1 = 1$, $n_2 = 0$, if the electron is at site 1, and $n_1 = 0$, $n_2 = 1$, if it is at site 2.

Using the transformation

$$q = Q_1 - Q_2; \quad Q_s = Q_1 + Q_2, \tag{B2}$$

the total energy now reads[26,55] as

$$E_{\rm tot} = \tfrac{1}{2}Kq^2 - \tfrac{1}{2}Vq(n_1 - n_2) + \left[-\tfrac{1}{2}VQ_s(n_1 + n_2) + \tfrac{1}{2}KQ_s^2\right]. \tag{B3}$$

Since always $n_1 + n_2 = 1$, the values in the second set of parentheses do not depend on the site of the electron. The first part, determined by the relative coordinate q, describes two parabolae, with the relative coordinate q as the abscissa

$$E = \tfrac{1}{2}Kq^2 \pm \tfrac{1}{2}Vq. \tag{B4}$$

Figure 7 shows these parabolae. The minima both lie below energy zero by

$$E_{\rm min} = \pm V^2/8K = \pm E_P/2, \tag{B5}$$

where E_P is the polaron stabilization energy in the Q_1 or the Q_2 coordinate system. The Franck-Condon type optical transition between both sites is shown by the vertical arrow. The energy of this transition $E_{\rm opt} = 2E_P$ is the energy difference of the electron at the final and the initial sites. It should be remarked that the electronic energy alone at the initial site is $-2E_P$ in the single site coordinate system. In the absence of the electron at the final site, the transition energy is then $2E_P$.

Thermal transitions between both sites are most probable if the lattice is thermally excited in such a way that the electronic energies at the initial and the final sites coincide: $1/2Vq = -1/2Vq$. This occurs at $q = 0$ [cf. Eq. (B4)], i.e., at the crossing of both parabolae. The thermal hopping transfer energy is thus [Eq. (B5)] $E_P/2$ [$= 0.27$ eV for free polarons in LN (Ref. 17)]. It is only by plotting the energies as depending on the common coordinate q that the thermal activation energy

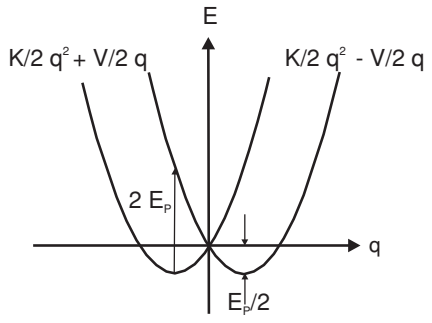

FIG. 7. Potentials related to two small polarons forming at two equivalent sites, as plotted over the relative coordinate $q = Q_1 - Q_2$.

for transitions between the involved sites can be read directly from such a diagram.

For two inequivalent polaron sites, such as Fe_{Li}^{2+} and Nb_{Nb}^{4+}, the total energy reads, correspondingly, as

$$E_{\rm tot} = E_1 + E_2 = KQ_1^2 - n_1V'Q_1 - n_1E_C + KQ_2^2 - n_2VQ_2. \tag{B6}$$

Here, E_C is the Fe defect-induced electronic energy at Fe_{Li}^{2+} and V' is the change (per unit distortion) of the electronic energy there. It is about 14% larger than V related to Nb_{Nb}^{4+}.[17] Transforming to the coordinates q and Q_s (see above), one obtains

$$E_{\rm tot} = \tfrac{1}{2}Kq^2 - \tfrac{1}{2}q(V'n_1 - Vn_2) - n_1E_C + \tfrac{1}{2}KQ_s^2 + \tfrac{1}{2}Q_s(V'n_1 + Vn_2). \tag{B7}$$

Neglecting the difference between V' and V, the terms containing Q_s are again independent of the position of the electron. Using the parameters derived in Ref. 17, $E_C = 1.22$ eV, $E_P = 0.54$ eV, and $E_P' = 0.70$ eV, one arrives then at the potential schemes in Figs. 4 and 5, dependent on the single relative coordinate q.

The thermal activation energy W_t for trapping the Nb_{Nb}^{4+} electron by the neighboring Fe_{Li}^{3+} can be calculated using an expression derived by Zylbersztejn[63] as formulated in the present nomenclature:

$$W_t = \frac{(2E_P - E_C)^2}{4(E_P + E_C)} \sim 0.004 \text{ eV}. \tag{B8}$$

This indicates that the trapping transition is practically not activated thermally, as mentioned in Sec. III B. We like to note that Zylbersztejn,[63] not knowing that the electronic ground state of reduced LN is of bipolaronic nature,[17] derived different parameters leading to the sizable trapping activation energy of 0.11 eV. On the basis of the present knowledge, this is not valid anymore.

The relative positions of the defect-dominated polaron levels (left part of Fig. 5) and the band states, determined by the periodic potential (right part of Fig. 5) at some distance from the defect, follow from the following considerations. The transferable electron at Fe_{Li}^{2+} is certainly localized at one site. This localization requires that Bloch waves of all **k** vectors interfere constructively at one site, leading to an increase of the kinetic energy E_k by typically half the width $E_k \sim 0.7$ eV of the conduction band[50] with respect to the lower conduction band edge (CBE). From this reference energy, the electron energy is lowered by both the local defect potential $E_C = 1.22$ eV and the polaron energy $E_P' = 0.70$ eV.[17] This localizes the electronic level at ~1.2 eV below the CBE. For comparison, the level of the Nb_{Li}^{4+} charge state of the antisite defect ($E_C = 0.53$ eV, $E_P' = 0.58$ eV) is predicted on this basis to ~0.4 eV below CBE, in line with the theoretical prediction by Nahm and Park.[39] Since the lowest energy threshold for electronic optical transitions from the valence band [in undoped CLN (congruently melting LN)] end in the Nb_{Li}^{5+} antisite defects, the energy difference between the Fe_{Li}^{2+} and the Nb_{Li}^{4+} levels, ~0.8 eV, is representative for the band

shift difference of Fe doped and undoped congruently melting LN. This difference was estimated by Clark *et al.*[20] to be ~0.6 eV. The peak of the Fe_{Li}^{2+} absorption band is predicted to lie at $2E_P' + E_C = 1.4$ eV+1.22 eV= 2.6 eV above the electronic ground state of Fe_{Li}^{2+}. These quantities define the energies indicated in Fig. 5.

*schirmer@uos.de

[1] A. M. Glass, D. von der Linde, and T. J. Negran, Appl. Phys. Lett. **25**, 233 (1974).
[2] K. Buse, Appl. Phys. B: Lasers Opt. **64**, 273 (1997).
[3] K. Buse, Appl. Phys. B: Lasers Opt. **64**, 391 (1997).
[4] M. Imlau, T. Bieringer, S. Odoulov, and T. Woike, in *Nanoelectronics and Information Technology* (Wiley, New York, 2003), p. 661.
[5] J. Feinberg, Opt. Lett. **7**, 486 (1982).
[6] R. Mueller, M. T. Santos, L. Arizmendi, and J. M. Cabrera, J. Phys. D: Appl. Phys. **27**, 241 (1994).
[7] L. Arizmendi, Phys. Status Solidi A **201**, 253 (2004).
[8] M. Qin, K. Yao, and Y. C. Liang, Appl. Phys. Lett. **95**, 022912 (2009).
[9] T. Choi, S. Lee, Y. J. Choi, V. Kiryukhin, and S.-W. Cheong, Science **324**, 63 (2009).
[10] S. Y. Yang, J. Seidel, S. J. Byrnes, P. Shafer, C.-H. Yang, M. D. Rossell, P. Yu, Y.-H. Chu, J. F. Scott, J. W. Ager III, L. W. Martin, and R. Ramesh, Nat. Nanotechnol. **5**, 143 (2010).
[11] B. I. Sturman and V. M. Fridkin, *The Photovoltaic and Photorefractive Effects in Noncentrosymmetric Materials* (Clarendon, Oxford, 1996).
[12] A. M. Glass, D. von der Linde, D. H. Auston, and T. J. Negran, J. Electron. Mater. **4**, 915 (1975).
[13] R. von Baltz, Phys. Status Solidi B **89**, 419 (1978).
[14] R. von Baltz and W. Kraut, Solid State Commun. **26**, 961 (1978).
[15] R. von Baltz, Ferroelectrics **35**, 131 (1981).
[16] H. Heyszenau, Phys. Rev. B **18**, 1586 (1978).
[17] O. F. Schirmer, M. Imlau, C. Merschjann, and B. Schoke, J. Phys. Condens. Matter **21**, 123101 (2009).
[18] Y. Qiu, K. B. Ucer, and R. T. Williams, Phys. Status Solidi C **2**, 232 (2005).
[19] S. Sasamoto, J. Hirohashi, and S. Ashihara, J. Appl. Phys. **105**, 083102 (2009).
[20] M. G. Clark, F. J. DiSalvo, A. M. Glass, and G. E. Peterson, J. Chem. Phys. **59**, 6209 (1973).
[21] N. S. Hush, Electrochim. Acta **13**, 1005 (1968).
[22] H. G. Reik, Solid State Commun. **1**, 67 (1963).
[23] H. G. Reik and D. Heese, J. Phys. Chem. Solids **28**, 581 (1967).
[24] D. M. Eagles, Phys. Rev. **130**, 1381 (1963).
[25] M. I. Klinger, Phys. Lett. **7**, 67 (1963).
[26] I. G. Austin and N. F. Mott, Adv. Phys. **18**, 41 (1969).
[27] D. Emin, Adv. Phys. **24**, 305 (1975).
[28] R. E. Peierls, *Quantum Theory of Solids* (Clarendon, Oxford, 1955).
[29] V. I. Belinicher and B. I. Sturman, Sov. Phys. Usp. **23**, 199 (1980) [Usp. Fiz. Nauk **130**, 415 (1980)].
[30] H. G. Festl, P. Hertel, E. Krätzig, and R. von Baltz, Phys. Status Solidi B **113**, 157 (1982).
[31] S. G. Odoulov, Ferroelectrics **91**, 213 (1989).
[32] V. M. Fridkin and R. M. Magomadov, Sov. Phys. JETP Lett. **30**, 686 (1979) [Pis'ma Zh. Eksp. Teor. Fiz. **30**, 723 (1979)].
[33] S. I. Karabekyan, Sov. Phys. Solid State **33**, 363 (1991) [Fiz. Tverd. Tela (Leningrad) **33**, 633 (1991)].
[34] S. I. Karabekyan and S. G. Odoulov, Phys. Status Solidi B **169**, 529 (1992).
[35] H. Kurz and E. Krätzig, Appl. Phys. Lett. **26**, 635 (1975).
[36] S. C. Abrahams, J. M. Reddy, and J. L. Bernstein, J. Phys. Chem. Solids **27**, 997 (1966).
[37] S. Juppe and O. F. Schirmer, Solid State Commun. **76**, 299 (1990).
[38] P. W. Atkins, *Molecular Quantum Mechanics* (Oxford University, Oxford, UK, 1983), p. 443.
[39] H. H. Nahm and C. H. Park, Phys. Rev. B **78**, 184108 (2008).
[40] R. Sommerfeld, L. Holtmann, E. Krätzig, and B. C. Grabmeier, Phys. Status Solidi A **106**, 89 (1988).
[41] O. F. Schirmer, S. Juppe, and J. Koppitz, Cryst. Lattice Defects Amorphous Mater. **16**, 353 (1987).
[42] C. Merschjann, B. Schoke, D. Conradi, M. Imlau, G. Corradi, and K. Polgar, J. Phys. Condens. Matter **21**, 015906 (2009).
[43] F. Jermann and J. Otten, J. Opt. Soc. Am. B **10**, 2085 (1993).
[44] B. Briat, V. G. Grachev, G. I. Malovichko, O. F. Schirmer, and M. Wöhlecke, in*Springer Series in Optical Sciences 114*, edited by P. Günter and J. P. Huignard (Springer, New York, 2007), p. 9.
[45] E. Krätzig and H. Kurz, Ferroelectrics **13**, 295 (1976).
[46] A. P. Levanyuk, A. R. Pogosyan, and E. M. Uyukin, Dokl. Akad. Nauk SSSR **256**, 60 (1981) [Sov. Phys. Dokl. **26**, 43 (1981)].
[47] A. P. Levanyuk, A. R. Pogosyan, E. M. Uyukin, and N. Z. Sarkisyan, Ferroelectrics **56**, 129 (1984).
[48] E. Krätzig and H. Kurz, Opt. Acta **24**, 475 (1977).
[49] A. R. Pogosyan, B. N. Popov, and E. M. Uyukin, Ferroelectrics **43**, 169 (1982).
[50] W. G. Schmidt, M. Albrecht, S. Wippermann, S. Blankenburg, E. Rauls, F. Fuchs, C. Rödl, J. Furthmüller, and A. Hermann, Phys. Rev. B **77**, 035106 (2008).
[51] X. X. Bi and P. C. Eklund, Phys. Rev. Lett. **70**, 2625 (1993).
[52] O. F. Schirmer, J. Phys. Condens. Matter **18**, R667 (2006).
[53] K. L. Sweeney and L. E. Halliburton, Appl. Phys. Lett. **43**, 336 (1983).
[54] D. A. Dutt, F. J. Feigl, and G. G. DeLeo, J. Phys. Chem. Solids **51**, 407 (1990).
[55] B. Faust, H. Müller, and O. F. Schirmer, Ferroelectrics **153**, 297 (1994).
[56] C. Merschjann, D. Berben, M. Imlau, and M. Wöhlecke, Phys. Rev. Lett. **96**, 186404 (2006).
[57] C. Merschjann, B. Schoke, and M. Imlau, Phys. Rev. B **76**, 085114 (2007).
[58] B. Sturman, M. Carrascosa, and F. Agullo-Lopez, Phys. Rev. B **78**, 245114 (2008).
[59] B. Sturman, J. Opt. Soc. Am. B **8**, 1333 (1991).
[60] W. Ruppel, R. von Baltz, and P. Würfel, Ferroelectrics **43**, 109 (1982).
[61] M. Qin, K. Yao, and Y. C. Liang, Appl. Phys. Lett. **93**, 122904 (2008).
[62] D. Emin, Phys. Rev. B **48**, 13691 (1993).
[63] A. Zylbersztejn, Appl. Phys. Lett. **29**, 778 (1976).